Boundary-Layer Meteorol (2007) 124:305–314
DOI 10.1007/s10546-007-9162-0

RESEARCH NOTE

A note on the top-down and bottom-up gradient functions over a forested site

Weiguo Wang · Kenneth J. Davis · Chuixiang Yi · Edward G. Patton · Martha P. Butler · Daniel M. Ricciuto · Peter S. Bakwin

Received: 22 March 2006 / Accepted: 23 January 2007 / Published online: 2 March 2007

Abstract The dimensionless bottom-up and top-down gradient functions in the convective boundary layer (CBL) are evaluated utilizing long-term well-calibrated carbon dioxide mixing ratio and flux measurements from multiple levels of a 447-m tall tower over a forested area in northern Wisconsin, USA. The estimated bottom-up and top-down functions are qualitatively consistent with those from large-eddy simulation (LES) results and theoretical expectations. Newly fitted gradient functions are proposed based on observations for this forested site. The integrated bottom-up function over the lowest 4% of the CBL depth estimated from the tower data is about five times larger than that from LES results for a 'with-canopy' case, and is smaller than that from LES results for a 'no-canopy' case by a factor of 0.7. We discuss the uncertainty in the evaluated gradient functions due to stability, wind direction, and uncertainty in the entrainment flux and show that while all of these have a significant impact on the gradient functions, none can explain the differences between the modelled and observed functions. The effects of canopy features and atmospheric stability may need to be considered in the gradient function relations.

W. Wang · K. J. Davis · M. P. Butler · D. M. Ricciuto
Department of Meteorology, The Pennsylvania State University, 503 Walker Building, University Park, PA 16802, USA

C. Yi
Department of Ecology, Evolutionary Biology, University of Colorado, Boulder, CO 80309, USA

E. G. Patton
Mesoscale and Microscale Meteorology Division, National Center for Atmospheric Research, P.O. Box 3000 Boulder, CO 80307, USA

P. S. Bakwin
Climate Monitoring and Diagnostics Laboratory R/CMDL1, National Oceanic & Atmospheric Administration, 325 Broadway, Boulder, CO 80305, USA

W. Wang (✉)
Pacific NW National Lab, K9-30, Richland, WA 99352, USA
e-mail: wang@met.psu.edu

Keywords Bottom-up diffusion · Convective boundary layer · Gradient functions · Observations · Top-down diffusion

1 Introduction

Observational studies indicate that potential temperature in the mixed layer is usually well mixed under clear-air and convective conditions while the water vapour mixing ratio is sometimes not well-mixed (Mahrt 1976). Wyngaard and Brost (1984) attempted to interpret the cause of this phenomenon, and argued that the mean mixing ratio profile of a passive, conserved scalar is determined by the scalar surface and entrainment fluxes, convective velocity scale, and convective boundary-layer (CBL) depth in horizontally homogeneous conditions. With dimensional analysis, they proposed top-down and bottom-up gradient functions to generalize the flux–gradient relationship in the CBL. The flux–gradient relationship is the basis of CBL parameterization in large-scale numerical models (e.g., Wyngaard 1984; Holtslag and Moeng 1991), and can be used to estimate the surface and entrainment fluxes of scalars from profile measurements (e.g., Davis 1992; Davis et al. 1994) or vice versa. For example, the CBL flux-gradient relationship might play a useful role in constraining regional carbon dioxide fluxes via mixing ratio measurements from towers, most of which are within the surface layer.

The gradient functions have been evaluated using large-eddy simulation (LES) in the CBL. For example, Wyngaard and Brost (1984) and Moeng and Wyngaard (1989) evaluated these functions for a horizontally homogeneous, canopy-free CBL, and Patton et al. (2003) studied the influence of a 25-m tall forest canopy (leaf area index (LAI) of 2) on top-down and bottom-up diffusion and re-evaluated the gradient functions in the presence of a plant canopy using a nested-grid LES model. These gradient functions, however, have not been previously quantitatively evaluated by observations due largely to the difficulty in obtaining mixing ratio profile measurements with sufficient instrumental precision and temporal averaging to discern small mean gradients in the presence of large convective fluctuations in the CBL (Davis 1992). In this study, we present estimates of the gradient functions calculated from well-calibrated measurements of carbon dioxide (CO_2) mixing ratios and fluxes at multiple levels on a very tall tower. The estimated functions are then compared with LES results and implications are discussed. Section 2 describes the experimental site and data. We use a bootstrap sampling method and solve linear equations involving the two gradient functions at different levels in Sect. 3. Results are presented in Sect. 4, and the analyses in Sect. 5 suggest that the CBL gradient functions are dependent not only on height but also on atmospheric stability and canopy features.

2 Experimental site and data

The 447-m tall communication tower (WLEF) (45.9° N, 90.3° W) is located about 15 km east of Park Falls, Wisconsin, USA. The region is relatively flat with mixed evergreen and deciduous forests; canopy height is about 20 m and LAI is about 3.4 with a standard deviation of 1.8 estimated from a MODIS (Moderate Resolution Imaging Spectroradiometer) product (Source: http://www.fsl.orst.edu/larse/bigfoot). The WLEF tower is part of the National Oceanographic and Atmospheric Administration's tall tower CO_2 monitoring network (Bakwin et al. 1998).

Vertical turbulent fluxes of momentum, sensible heat, latent heat, and CO_2 are measured with the eddy-covariance technique at three levels (30, 122, and 396 m above the ground level) of the tower (Berger et al. 2001; Davis et al. 2003); CO_2 mixing ratio data, traceable to World Meteorological Organisation primary standards, are collected at six levels (11, 30, 76, 122, 244, and 396 m) (Bakwin et al. 1998; Davis et al. 2003). The CO_2 mixing ratio measurements are made with a single infrared gas analyzer that samples air from multiple inlets using an automated switching mechanism (Bakwin et al. 1998), and which eliminates systematic errors due to instrumental offset. Mixing ratio measurements were initiated in 1994, and flux measurements in 1995, and this long record of extended vertical profiles of CO_2 fluxes and mixing ratios is unique globally. A 915 MHz boundary-layer profiler radar was deployed in the region in 1998 and 1999, and reflectivity profiles from the radar were used to derive the mixed-layer depth (Angevine et al. 1994; Yi et al. 2001). Hourly-averaged CO_2 turbulent fluxes, CO_2 mixing ratio profiles, and CBL depth collected from May to September in 1998 and 1999 are used in the following analyses because the radar data are primarily available only during this period. The CBL depth ranges approximately from 380 to 2000 m, with the CBL well developed under fair weather conditions (Yi et al. 2001). Approximately 50% of the available data (477 h) were measured under strongly unstable conditions ($L/h > -0.1$, where L is the Obukhov length, h is the CBL depth) (Fig. 1). Approximately 22%, 21%, 30%, and 27% of the available measurements were made with winds from the north-east (NE), south-east (NE), south-west (SW), and north-west (NW) directions, respectively. Mean wind speeds at the 396-m level of the tower were about 7, 10, 10, and 8 m s^{-1} for the four wind directions, respectively, during these hours.

3 Theory and method

The top-down and bottom-up diffusion hypothesis is described in detail by Wyngaard and Brost (1984) and Wyngaard (1987). Wyngaard and Brost (1984) presented a similarity hypothesis and proposed the following equation to describe the mean

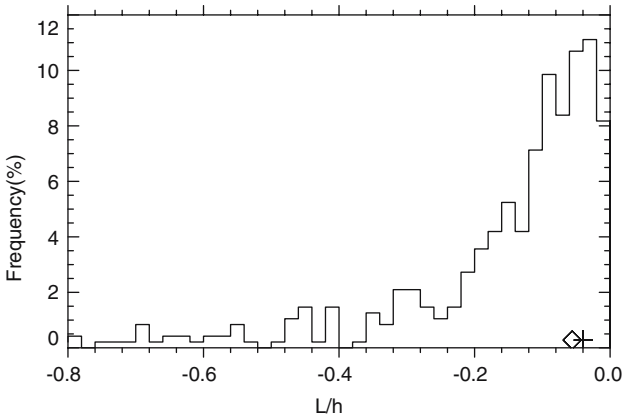

Fig. 1 Distribution of atmospheric stability (expressed as the ratio of L to h) under which the gradient functions are fitted using data from 447 h. The frequency of data with $L/h < -0.8$ is about 4%. The median value of L/h is −0.104. Diamond and plus signs indicate the L/h values of Patton et al. (2003) LES experiments for with-canopy and no-canopy conditions, respectively

(passive, conserved) scalar mixing ratio gradient as the sum of bottom-up and top-down components in the CBL,

$$\frac{\partial C}{\partial z} = -g_b\left(\frac{z}{h}\right)\frac{\overline{wc}_0}{hw_*} - g_t\left(\frac{z}{h}\right)\frac{\overline{wc}_h}{hw_*}, \tag{1}$$

where C is the mean mixing ratio of the scalar, $\overline{wc}_0$ and $\overline{wc}_h$ are the turbulent scalar surface and entrainment fluxes, respectively, z is the altitude above the surface, and g_b and g_t are dimensionless bottom-up and top-down gradient functions of dimensionless height within the CBL; w_* is the convective velocity scale ($= [gQ_sh/\theta_0]^{1/3}$), where θ_0 and Q_s are the mean virtual potential temperature and heat flux at the surface, respectively, and g is the gravitational acceleration. Three assumptions were made in this scaling argument. Firstly, differential advection (in the vertical) is negligible. Secondly, the convective layer parameters (CBL depth, convective velocity scale, scalar surface and entrainment fluxes) vary slowly compared to the convective turnover time (h/w_*) (i.e., the quasi-steady state assumption). Finally, the boundary layer is highly convective. Wyngaard and Brost (1984) argued that the above assumptions are not restrictive in many applications. Davis (1992) explored the range of these assumptions and found them to be fairly robust for daytime conditions.

We select the CBL depth (h) to scale the altitude. To use multi-level CO_2 mixing ratio measurements on the tall tower, we partition the entire CBL vertically into n equal intervals; the dimensionless length of each interval is $\delta = 1/n$, the dimensionless altitudes of mesh points are $Z_0 = 0, Z_1 = \delta, Z_2 = 2\delta, \ldots, Z_n = n\delta = 1$, where Z_i (i: from 0 to n) is the ith mesh point, and Z_0 and Z_n are the dimensionless altitudes of the surface and the mixed-layer top, respectively. The mean gradient functions $G_b(i)$ and $G_t(i)$ over the ith interval from $Z_i = i\delta$ to $Z_{i+1} = Z_i + \delta$ are,

$$G_b(i) = \frac{1}{\delta}\int_{Z_i}^{Z_i+\delta} g_b\,(Z)dZ, \tag{2}$$

and,

$$G_t(i) = \frac{1}{\delta}\int_{Z_i}^{Z_i+\delta} g_t\,(Z)dZ. \tag{3}$$

With (2) and (3), the mean mixing ratio difference at time t over a dimensionless altitude interval from Z_j to $Z_k (j < k)$, therefore, can be expressed by integrating Eq. 1,

$$\begin{aligned} C(Z_k,t) - C(Z_j,t) &= -\frac{\overline{wc}_0(t)}{w_*(t)}\int_{Z_j}^{Z_k} g_b\,(Z)\,dZ - \frac{\overline{wc}_h(t)}{w_*(t)}\int_{Z_j}^{Z_k} g_t\,(Z)\,dZ \\ &= -\frac{\overline{wc}_0(t)}{w_*(t)}\delta\left[G_b(j) + G_b(j+1) + \cdots + G_b(k-1)\right] \\ &\quad -\frac{\overline{wc}_h(t)}{w_*(t)}\delta\left[G_t(j) + G_t(j+1) + \cdots + G_t(k-1)\right]. \end{aligned} \tag{4}$$

Given measurements of (a) CO_2 mixing ratio at different levels, (b) h, (c)w_*, (d) scalar surface fluxes, and (e) entrainment fluxes at various times, we obtain a set of linear equations involving G_b and G_t. If the number of the equations is equal to or greater than the number of unknowns ($2n$), G_b and G_t can possibly be estimated by directly solving the linear equations or by fitting an optimal solution with the least-squares method.

To consider the impacts of the canopy, a displaced vertical coordinate, $(z - d)/h$, is used, where d is the zero-plane displacement height for momentum; this coordinate is used for comparing our results to LES results of Patton et al. (2003). Under convective conditions, CO_2 fluxes at three levels of the tower are extrapolated to the effective surface and top of the CBL with the assumption of a linear flux profile, giving estimates of the surface and entrainment fluxes. The first, second, and third quartiles of the magnitude of the ratio of the entrainment flux to surface flux are 0.84, 2, and 5.7, respectively, for the analyzed hours in this study. CO_2 mixing ratio profile data provide the mean mixing ratio differences between levels (i.e., left-hand side of Eq. 4). The dimensionless heights of the CO_2 mixing ratio measurements (scaled by $h(t)$) are rounded to the closest mesh points (Z_i). The convective velocity scale,w_*, is calculated based on the measurements of the virtual potential temperature and its vertical flux at the 30-m level on the tower, and the CBL depth.

4 Results

The zero-plane displacement height and aerodynamic roughness length are 16 m and 0.9 m during the summer (June through August), respectively, estimated under *nearly neutral* conditions by fitting measured wind speeds at 30 m and 122 m to the logarithmic wind profile. In the early and late growing season (May and September), the two variables are 15 m and 0.6 m, respectively. The CO_2 mixing ratio at the effective surface level is estimated with a quadratic polynomial fit to CO_2 mixing ratios from the six levels. We calculate the differences (i.e., left-hand side of Eq. 4) in CO_2 mixing ratios between the effective surface level and other higher levels. The total number of available linear equations (i.e., Eq. 4) is 1609. To estimate the uncertainty of the calculation, we adopt a bootstrap sampling method (Efron and Tibshirani 1993; Davison and Hinkley 1997), where we randomly resample the equations with replacements (from the 1609 equations) for 2000 times with each sample being the same size as the original sample (i.e., 1609 equations). Then the optimal solutions for G_b and G_t are estimated by minimizing the residual error of each re-sampled equation set in a least-squares sense. The 90% confidence intervals are constructed by finding the 5th and 95th percentiles of the solutions at each level for the bootstrapping equation sets. The gradient functions are evaluated in the lower half of the CBL with $\delta = 0.04$ and in the whole CBL with $\delta = 0.1$, respectively. The lower resolution is used for the latter case since data are sparse in the upper part of the CBL.

Figure 2 presents the median values and 90% confidence intervals of the estimated mean gradient functions over each interval (G_b and G_t, filled circles) varying with dimensionless height. The results are plotted at the midpoint of each interval, i.e., $Z_i + 0.5\delta$. The median value of G_b is about 118 over the interval from the roughness height (above the zero-plane displacement height) to 4% of the CBL depth, and decreases rapidly with height. G_b is close to zero (Fig. 2a) when the effective altitude $(z - d)$ is higher than 20% of the CBL depth, suggesting a higher mixing efficiency. In the lower half of the CBL, top-down transport is highly efficient (G_t is close to zero, Fig. 2b). G_b tends to be negative at higher levels of the CBL, as suggested by Moeng and Wyngaard (1989), but the results are very scattered. The variation of the functions with height is qualitatively consistent with theoretical expectations (Wyngaard and Brost 1984) and LES results (Wyngaard and Brost 1984; Moeng and Wyngaard 1989; Patton et al. 2003).

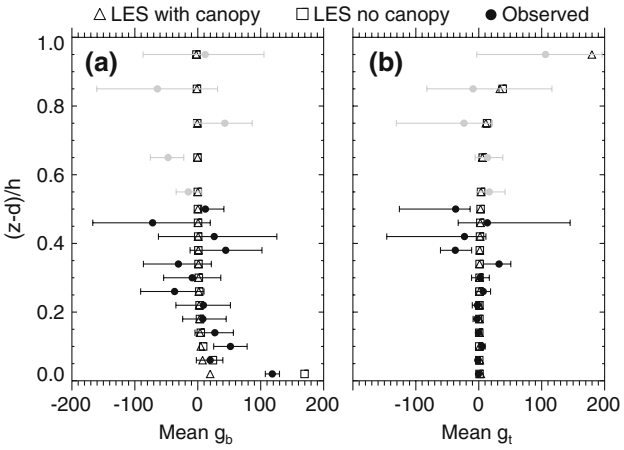

Fig. 2 The median, 5% and 95% percentiles of the mean bottom-up (**a**) and top-down (**b**) functions over each interval derived from the tower data (filled circles). Black filled circles represent the results in the lower half part of the mixed layer estimated using a resolution of $\delta = 0.04$. Gray filled circles represent results in the upper half of the mixed layer using a resolution of $\delta = 0.1$. Results from LES (Patton et al. 2003) are shown by triangles (with-canopy case) and squares (no-canopy case)

Assuming that the gradient functions are smoothly varying, we fit the results (Fig. 2) using power-law functions as adopted in the literature. If we interpret the mean gradient functions (G_b and G_t) as g_b and g_t functions at the altitude of the mid-point of each interval, good fits of the g_b and g_t functions to the median values estimated from the tower data at each level are

$$g_b(z) = 1.06\left(\frac{z-d}{h}\right)^{-1.20}, \tag{5}$$

and,

$$g_t(z) = 0.12\left(1-\frac{z-d}{h}\right)^{-2.27}. \tag{6}$$

The fitted functions suggest that transport from the mixed-layer top and bottom may be asymmetric (Fig. 3). When $(z-d)/h$ is smaller than 20%, $g_t(1-(z-d)/h)$ is greater than $g_b((z-d)/h)$, suggesting that mixing is more efficient in the region near the bottom than near the top of the mixed layer. When $(z-d)/h$ is larger than 20%, both $g_b((z-d)/h)$ and $g_t(1-(z-d)/h)$ functions are small (< 10), and g_t is smaller than g_b. It should be pointed out here that the fitted expressions represent the gradient functions averaged over the stability range of the available observations for this specific site during the growing season.

5 Comparisons and discussion

This section compares the estimated gradient functions from the tall-tower data with those from two LES experiments reported in the literature. We also compare the gradient functions derived from the tower data under different conditions.

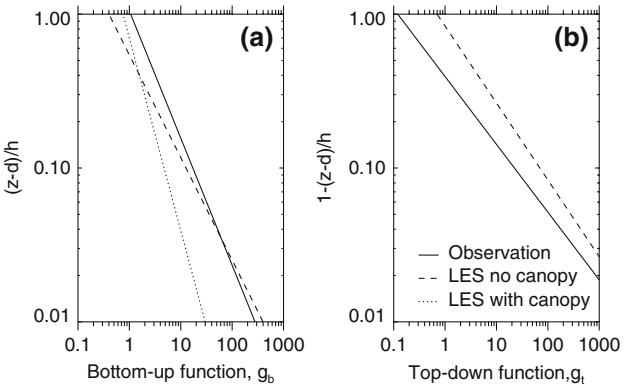

Fig. 3 g_b (**a**) and g_t (**b**) functions fitted to LES results and to tower data (solid lines). Fitted LES results are shown by dashed lines (no-canopy case) and dotted line (with-canopy case) (Patton et al. 2003). The LES g_t function for the no-canopy case is nearly same as that for the with-canopy case

5.1 Comparisons with the gradient functions estimated from two LES experiments

Patton et al. (2003) used a nested-grid capable LES model to evaluate the gradient functions in a horizontally homogenous CBL for with-canopy and no-canopy conditions, respectively. The nested grid system was used to resolve small-scale turbulence near the surface as well as the impacts of a 25-m tall plant canopy. Three passive and conservative scalars were added to the LES model to evaluate differences in top-down and bottom-up diffusion processes. Two of the scalars were used to calculate the gradient functions. One scalar represented pure top-down diffusion, which had zero surface flux and its only source was through entrainment. The top-down gradient function (g_t) was calculated from the distribution of the scalar. The other scalar had both surface and entrainment-induced fluxes, and, therefore, represented combined top-down and bottom-up diffusion. The entrainment contribution was removed using the calculated g_t and hence the g_b function was calculated from the vertical distribution of the second scalar using Eq. 1. All statistics were averaged over the horizontal plane and over about three large-eddy turnover times. The gradient functions were estimated when the stability parameter, L/h,was equal to -0.056 for the with-canopy condition, and -0.04 for the no-canopy condition.

We compare the mean g_b and g_t values over each interval calculated from the tower data with those from the above two LES experiments (triangle and squares in Fig. 2). LES results of Patton et al. (2003) suggest that the bottom-up gradient function with the presence of a canopy is significantly smaller through the region below $0.1(z-d)/h$ (Fig. 2a) than that without the canopy. Our results, however, show that the estimated G_b function from tower data is intermediate and closer to the LES results for the no-canopy case than for the with-canopy case. In the lower part of the CBL, G_t values derived from LES and the tower data are not statistically significantly different. The fitted gradient functions are compared in Fig. 3. The g_b values derived from the tower data lie between those derived from LES with and without the plant canopy below $0.03h$, while larger than both LES-derived g_b values above $0.03h$. The g_t values fitted from the tower data are smaller than those derived from both LES experiments.

5.2 Discussion

Patton et al. (2003) found that the gradient functions are dependent on canopy features and suggested that such dependence cannot be fully described by introducing a zero-plane displacement height into the relations for the gradient functions. This could be one of the reasons explaining the differences in the gradient functions evaluated from LES and from the tower data because canopy features in the tower area (e.g., LAI = 3.4) are different from those in both LES experiments (LAI = 2 and 0), though it is hard to explain why the larger LAI around the tower would yield G_b near the surface between the LES results.

Patton et al. (2003) also suggested that the functions might depend on atmospheric stability, which is reasonable given that the original discussion of the gradient functions (Wyngaard and Brost 1984) was limited to strongly unstable conditions. Additional factors that could influence our results are variations in canopy structure as a function of wind direction, and errors in our measurements of the entrainment and surface fluxes. We test theses factors by breaking down the available observations into appropriate groups. In each case, we limit our comparison to G_b values in the lowest interval (near the surface) due to large error bounds in the higher levels.

We first compare strongly unstable condition ($-0.1 < L/h < 0$) to weakly unstable conditions ($L/h \leq -0.1$), and the gradient functions are recalculated using data from each category. The G_b values in the lowest interval are about 125 ± 10 and 103 ± 12 (hereafter, the error bar represents one standard deviation of the estimated G_b) for the weakly and strongly unstable conditions, respectively. The former is slightly larger than the latter (68% confidence). This comparison implies that the gradient functions may vary not only with dimensionless height but also with atmospheric stability, lending support to the Patton et al. (2003) suggestion. The LES results were obtained under strongly convective conditions, while the tower results in Fig. 2 were obtained from all data available under unstable conditions ($-1 < L/h < 0$). Due to the limited data and large uncertainty, we are unable to provide a modification that incorporates a stability parameter into the current gradient function relations based on these results. This stability dependence moves our results towards the with-canopy LES results, but does not resolve the large discrepancy.

Surface heterogeneity may affect scalar transport and mixing in the CBL, and might account in part for large scatter of the evaluated gradient functions. We evaluate the functions using data from different wind directions to test for variability due to the effects associated with surface heterogeneity. We break down the data into four groups in which the wind direction is from the NE, SE, SW, and NW directions, respectively, noting that wind direction and stability are not significantly correlated. The gradient functions are recalculated for each data group. The G_b values in the lowest interval are about 90 ± 9 and 122 ± 10 when the wind is from the NE or SE direction and from the SW or NW direction, respectively. While this does suggest potential dependence on surface conditions, the dependence of fluxes on wind direction at the site is weak (Davis et al. 2003), and the differences in G_b between observations and the LES are significant regardless of wind direction.

The entrainment flux is estimated from three-level flux measurements in the lower CBL. To estimate the importance of the uncertainty in the entrainment flux, we break down the data into two groups based on the ratio of the estimated entrainment flux to surface flux and recalculate the functions. One group includes data when the magnitude of this ratio ≤ 2; approximately 50% of the data fall into this group. For these

data, G_b in the lowest interval is about 102 ± 8. The other group includes data with the magnitude of the ratio > 2, and where G_b in the lowest interval is 131 ± 10. The different flux ratio groups have no significant dependence on wind direction and stability. Given that the gradient functions for passive scalars are independent of the surface and entrainment fluxes as originally proposed, the difference in G_b under the different flux ratios may be mainly due to errors in the estimated entrainment flux. The large flux ratio implies relatively small surface fluxes, thus perhaps poorer constraint on the bottom-up gradient function.

Finally, LES-derived gradient functions near the surface are the most dependent on the subgrid-scale flux parameterization that is still uncertain. This might also partly account for the difference between results from LES data and from the tower data. None of the sources of uncertainty or variability in our estimated G_b values that we were able to assess can reconcile the discrepancy between LES results and the tower-derived functions.

6 Concluding remarks

We use multi-level observations of CO_2 mixing ratios and fluxes at the WLEF tower to estimate the mean bottom-up and top-down gradient functions under convective conditions. A bootstrap sampling method is used to evaluate the confidence intervals for our estimates. Bottom-up mixing is much more efficient (G_b is much smaller) above the surface layer than within the surface layer. In the lower part of the CBL, the top-down function derived from the tower data is small. Newly fitted functions are proposed by fitting the data under unstable conditions ($-1 \leq L/h < 0$) for this forested site during the growing season. The bottom-up function near the surface estimated from the tower data falls between the LES results for no-canopy and with-canopy conditions, despite the LAI in the region of the tower being larger than either LES scenario. We evaluate the dependence of the functions on atmospheric stability, wind direction, and entrainment to surface flux ratio. We find significant differences in each case, but none is large compared to the discrepancy between observed and LES-derived G_b values in the lowest layer of the CBL. How to incorporate canopy and stability effects into the gradient function relations requires further investigating in order to make them applicable more widely. Comparisons between the LES and tower-derived gradient functions in the mid-CBL are inconclusive since the gradient functions are very small and uncertainty in the values derived from the tower data is large. Additional observations at this site and other tall towers would help to reduce uncertainty in the gradient functions. Remote sensing (e.g. Doppler lidar and differential absorption lidar) may provide another means to obtaining more conclusive observations, though height-dependent biases in the data would need to be very small.

Acknowledgements This work was funded in part by Department of Energy Office of Biological & Environmental Research Terrestrial Carbon Program and National Science Foundation Collaboration Network grant DEB-0130380. The authors thank Roger Strand (chief engineer for WLEF-TV) and the Wisconsin Educational Communications Board, the University of Wisconsin's Kemp Natural Resources Station, and Ron Teclaw of the USDA Forest Service for additional support of this research.

References

Angevine WM, White AB, Avery SK (1994) Boundary-layer depth and entrainment zone characterization with a boundary-layer profiler. Boundary-Layer Meteorol 68(4):375–385

Bakwin PS, Tans PP, Hurst DF, Zhao C (1998) Measurements of carbon dioxide on very tall towers: results of the Noaa/cmdl program. Tellus Ser B-Chem Phys Meteorol 50(5):401–415

Berger BW, Davis KJ, Yi C, Bakwin PS, Zhao CL (2001) Long-term carbon dioxide fluxes from a very tall tower in a northern forest: flux measurement methodology. J Atmos Ocean Technol 18(4):529–542

Davis KJ (1992) Surface fluxes of trace gases derived from convective-layer profiles, Ph.D. Thesis. University of Colorado, Boulder, CO, 281 pp

Davis KJ, Bakwin PS, Yi C, Berger BW, Zhao C, Teclaw RM, Isebrands JG (2003) The annual cycles of CO_2 and H_2O exchange over a Northern mixed forest as observed from a very tall tower. Global Change Biol 9(9):1278–1293

Davis KJ, Lenschow DH, Zimmerman PR (1994) Biogenic nonmethane hydrocarbon emissions estimated from tethered balloon observations. J Geophys Res-Atmos 99(D12):25587–25598

Davison AC, Hinkley DV (1997) Bootstrap methods and their application. Cambridge University Press, Cambridge, UK, 582 pp.

Efron B, Tibshirani R (1993) An introduction to the bootstrap. Chapman & Hall, New York, 436 pp

Holtslag AAM, Moeng C-H (1991) Eddy diffusivity and countergradient transport in the convective atmospheric boundary layer. J Atmos Sci 48(14):1690–1698

Mahrt L (1976) Mixed layer moisture structure. Mon Wea Rev 104(11):1403–1407

Moeng CH, Wyngaard JC (1989) Evaluation of turbulent transport and dissipation closures in 2nd-order modeling. J Atmos Sci 46(14):2311–2330

Patton EG, Sullivan PP, Davis KJ (2003) The influence of a forest canopy on top-down and bottom-up diffusion in the planetary boundary layer. Quart J Roy Meteorol Soc 129(590):1415–1434

Wyngaard JC (1984) Toward convective boundary layer parameterization: a scalar transport module. J Atmos Sci 41(12):1959–1970

Wyngaard JC (1987) A physical-mechanism for the asymmetry in top-down and bottom-up diffusion. J Atmos Sci 44(7):1083–1087

Wyngaard JC, Brost RA (1984) Top-down and bottom-up diffusion of a scalar in the convective boundary layer. J Atmos Sci 41(1):102–112

Yi C, Davis KJ, Berger BW, Bakwin PS (2001) Long-term observations of the dynamics of the continental planetary boundary layer. J Atmos Sci 58(10):1288–1299